Infrared spectrum and structure of the

homochiral serine octamer - dichloride complex

Jongcheol Seo[1]*, Stephan Warnke[1], Kevin Pagel[1,2], Michael T. Bowers[3] and Gert von Helden[1]*

[1] Fritz-Haber-Institut der Max-Planck-Gesellschaft, Faradayweg 4-6, 14195 Berlin, Germany

[2] Freie Universität Berlin, Institute of Chemistry and Biochemistry, Takustrasse 3, 14195 Berlin, Germany.

[3] Department of Chemistry and Biochemistry, University of California Santa Barbara, Santa Barbara, California 93106, United States.

* e-mail: jseo@fhi-berlin.mpg.de (J.S.), helden@fhi-berlin.mpg.de (G.v.H.)

Abstract

The amino acid serine is known to form a very stable octamer which has properties that sets it apart from serine complexes having different sizes or from complexes composed of other amino acids. For example, both singly protonated serine octamers and anionic octamers complexed with two halogen ions, strongly prefer homochirality even when assembled from racemic D, L mixtures. Consequently, the structures of these complexes are of great interest but no acceptable candidates have so far been identified. Here we investigate anionic serine octamers coordinated with two chloride ions using a novel ion mobility/infrared spectroscopy technique in combination with theoretical calculations. The results allow the identification of a unique structure for $(Ser_8Cl_2)^{2-}$ that is highly symmetric, very stable, homochiral and whose calculated properties match those observed in the experiments.

Clusters of atoms or molecules with unusually high relative intensities in mass spectra are termed "magic". In many instances, those "magic" clusters could be assigned to specific structures, often of high symmetry. Examples are numerous and include rare gas clusters[1], fullerenes, most notably C_{60},[2] Ti_8C_{12} "metallocarbohedrane",[3] metal clusters such as Au_{20},[4,5] and highly symmetric protonated water clusters.[6,7] In the case of C_{60}, the initial observation of magic numbers in mass spectra eventually led to the discovery of a new group of materials and a new form of carbon. Occasionally a "magic" cluster resists structural characterization. A famous example is the serine octamer. After electrospray of solutions containing serine, it was first observed that a cluster with the composition $(Ser_8H)^+$ dominated the mass spectrum.[8] This is in contrast to mass spectra of other amino acid clusters, for which the intensity patterns of peaks in their mass spectra show much smoother evolution.[9-14] Moreover, it was observed that when performing experiments with solutions containing a 50:50 mixture of L-serine and D-serine, the serine octamer defies statistics by strongly preferring homochiral clusters, i.e. octamers that exclusively contain L-serine or D-serine.[15] Because of this unusual property, a possible link to the origin of homochirality in living organisms was made.[16] Besides $(Ser_8H)^+$, several other cationic serine octamer clusters, such as $(Ser_8Na)^+$, were found to show "magic" behavior.[17] For anionic clusters, a deprotonated octamer has not been reported to show signs of special behaviour. However, octamer clusters containing two halide ions such as $(Ser_8Cl_2)^{2-}$ and $(Ser_8Br_2)^{2-}$ are found to be abundant in mass spectra and further, are observed to prefer homochirality as well.[18] For anionic clusters of other amino acids, a special behavior similar to that of $(Ser_8Cl_2)^{2-}$ or $(Ser_8Br_2)^{2-}$ is again not observed.[18]

The experimental observations have spurred calculations, and several candidates for structures of cationic serine octamers have been proposed.[8,17,19-21] However, for most of them, the proposed structures do not provide an obvious reason for the observed homochirality. In addition, while the calculations indicate that the proposed structures are stable, they are not dramatically more stable compared to serine clusters of different sizes. Thus, there is no general consensus of the structure of serine octamer clusters and the quest for finding a structure that is compatible with the experimental observations is still ongoing.

In contrast to the abundance of studies on the cationic serine octamer, little attention has so far been given to the anionic species. Here, we present results from a study on serine cluster anions, in which we couple ion mobility-mass spectrometry (IMS-MS) with infrared (IR) spectroscopy. IMS-MS gives the absolute, angle averaged collision cross section (CCS) of specific clusters and this value can be used to determine the overall size of the cluster and to judge if particular calculated structures are compatible with the experiment.[22-24] Further, IM-MS can be used to prepare samples for gas-phase IR spectroscopy.[25-29] Here ions are simultaneously mass-to-charge (m/z) selected by MS and specific oligomers are geometrical size selected by IMS. This is in contrast to experiments where only m/z selection is used which can suffer from signal overlap between a cluster and its larger counterpart, which, for example, have twice the mass and twice the charge. While IMS provides information on the size and shape of a cluster, IR spectroscopy, especially in the fingerprint region (1000–2000 cm^{-1}), provides insights into the nature and interactions of functional groups in amino acids. IR spectroscopy without the use of IMS has been used to study the cationic protonated serine octamer with various substitutions in the X-H stretching region (X = N or O; 3000–4000 cm^{-1}), however not yielding a definite structure for this complex.[30-32] The focus of this study lies on $(Ser_8Cl_2)^{2-}$ for which a structure with high symmetry and stability is proposed. This structural assignment is supported by the experimental results as well by *ab-initio* calculations and we speculate that this complex might also exist in the condensed phase.

Results and Discussion

Figure 1 shows time-of-flight (TOF) mass spectra as well as IMS-resolved TOF mass spectra after electrospray of three serine samples. In Fig. 1a) the mass spectrum of an L-Ser sample is shown. The strongest peak occurs at m/z 455. Its drift time distribution (Fig. 1d) has a single peak that results from clusters with the composition $(Ser_8Cl_2)^{2-}$ with no indication of the presence of isomers or higher oligomers (such as quadruply charged 16-mers). In the 2-D plot in the lower part of Fig. 1a), all peaks for higher m/z species clearly group into different families that can be assigned to doubly and triply charged clusters. From the peaks in the drift time distributions collision cross sections (CCS) can be calculated and are given in Supplementary Table 1. No

clusters containing less than eight serine molecules are observed. The intensity of the cluster containing nine serine molecules is very weak, but larger clusters that range in composition from $(Ser_{10}Cl_2)^{2-}$ to $(Ser_{28}Cl_3)^{3-}$ are observed.

In Fig. 1b) the mass spectrum for a sample of 1:1 D-Ser and L-Ser is shown. Clearly, significant differences from the enantiomerically pure sample in Fig. 1a) are observed. Most importantly, the relative intensities in the mass spectrum are different. The largest peak is now $(Ser_{10}Cl_2)^{2-}$ and the octamer $(Ser_8Cl_2)^{2-}$ has decreased in relative intensity. The drift time distribution for the octamer at m/z = 455 has two peaks at drift times of ~5.9 ms and ~6.3 ms (labeled **I** and **II**, respectively) with the composition $(Ser_8Cl_2)^{2-}$ and cross sections of 189 $Å^2$ and 201 $Å^2$, respectively.

An interesting question is how L- and D-Ser are distributed in the clusters for the 1:1 mixture. To answer this, experiments using D-Ser and isotopically labeled L-Ser* that is heavier by 7 amu were performed. The mass spectra and 2-D plots are presented in Fig. 1c) and f). The mass spectrum on the top of Fig. 1c) shows broad peaks that arise from a heterogeneous distribution of L-Ser* and D-Ser within each cluster. Most peaks appear to be symmetrical bell-shaped, suggestive of clusters with a statistical distribution of L-Ser* and D-Ser. However, the distribution centered at m/z 469 is very different and does not have a bell shape. In the 2-D drift time vs. m/z plot in Fig. 1c), one can observe that several drift time peaks fall into that m/z region and they are labeled **I**, **II** and **III**. Peak **I** appears at the same drift time as peaks **I** in Figs. 1a) and b) and peak **II** at the same position as peak **II** in Fig. 1b). Peak **III** on the other hand is new. The mass spectra corresponding to drift time peaks **I**, **II** and **III** are shown in Fig. 1f). The mass spectrum for peak **I** shows a clearly non-statistical distribution of L-Ser* and D-Ser with the maxima at m/z 455 and 483 corresponding to clusters where all eight Ser molecules are D-Ser (0+8) and L-Ser* (8+0), respectively. Next to the maxima are partially resolved and weaker peaks that correspond to the 1+7 and 7+1 clusters. Mass peaks that correspond to 2+6 (6+2), 3+5 (5+3) or 4+4 clusters are not observed for drift time peak **I**. (It should be noted that for the case of a statistical assembly, the probability of randomly producing an 8+0 or 0+8 cluster is only 0.004, compared to a

probability of 0.27 for the 4+4 cluster). Peak **II** in Fig. 1f) hand looks different than Peak **I** and appears more bell-shaped with a maximum at *m/z* 469, corresponding to the 4+4 cluster. Peak **III** has a mass spectrum identical to peak **II**. This is strong evidence that this peak originates from loss of a Ser molecule from $(Ser_9Cl_2)^{2-}$ after the drift region but before *m/z* selection. This is not unexpected given the apparently weak binding energy of a Ser molecule to the core $(Ser_8Cl_2)^{2-}$ cluster. The results from the IMS-MS experiment thus clearly show that when both L-Ser and D-Ser are present, $(Ser_8Cl_2)^{2-}$ strongly prefers a compact structure that is homochiral in spite of the statistical improbability of this result. The statistically favored non-homochiral structure (peak **II**) is formed as well, however its structure is different and significantly less compact. A non-homochiral isomer is also observed for the cationic protonated octamer,[33] however, ion mobility experiments have not reported the presence of different isomers for those species.[20,21]

In order to gain more insight into the structure of the serine octamer, we performed IR spectroscopy on $(Ser_8Cl_2)^{2-}$ as well as $(Ser_{10}Cl_2)^{2-}$ and $(Ser_{12}Cl_2)^{2-}$ using samples of both pure L-Ser and 1:1 chirally mixed L-Ser and D-Ser. The IR spectra of the *m/z* and drift time-selected species, together with the corresponding drift time distributions are shown in Fig. 2. The red trace in Fig. 2c) shows a drift time distribution of $(Ser_8Cl_2)^{2-}$ of pure L-Ser where only a single peak is observed, as expected. The IR spectrum associated with this peak is shown in the lower red trace of Fig. 2f). The strongest IR band is found at 1637 cm^{-1}, which has a shoulder at lower wavenumbers. Further strong bands are observed at 1496 cm^{-1}, 1382 cm^{-1} and 1059 cm^{-1}.

When a 1:1 L-Ser and D-Ser sample is sprayed, the drift time distribution for the *m/z* 455 channel, corresponding to $(Ser_8Cl_2)^{2-}$ contains two peaks and is shown in the blue trace of Fig. 2c). The CCS of peak **I** (189 Å^2) is the same as for the peak in red for the pure L-Ser and is thus due to homochiral $(Ser_8Cl_2)^{2-}$. Peak **II**, on the other hand, originates from a less compact structure (CCS = 201 Å^2) , which is statistically assembled from L-Ser and D-Ser and not homochiral. The IR spectra resulting from peaks **I** and **II** are shown in the two blue traces in Fig. 2f). The bands in the IR spectrum of the $(Ser_8Cl_2)^{2-}$ ions that give rise to peak **I** occur at the same position and have a comparable width, compared to those observed in the spectrum of the pure L-Ser sample

in red. The spectrum for peak **II**, on the other hand, has bands at similar positions, but all of them are significantly broader. All IR spectra in Fig. 2) are taken using the same IR laser settings and hence any saturation effects or power broadening would affect all spectra the same way.

Figs. 2a) and 2b) show drift time distributions for the larger clusters and Figs. 2d) and 2e) their corresponding IR spectra. In all drift time distributions only a single peak is observed and all their IR spectra are very similar and consist of broad bands, analogous to the spectrum for peak II of $(Ser_8Cl_2)^{2-}$.

A qualitative assignment of the spectra can give information on the structures of the clusters, even without performing quantum chemical calculations. For isolated amino acid molecules in the gas phase, structures with neutral carboxylic acid and amine groups are most stable. In aqueous solution, on the other hand, the zwitterionic form is more stable. To help answer the question which form exists in the serine clusters, the vibrational modes of the carboxylic acid are most diagnostic. The band for the C=O stretch mode of a neutral carboxylic acid should occur for a free acid around 1780 cm^{-1} [34] and shifts to 1710 cm^{-1} when strongly hydrogen bonded to another acid[35] or 1727 cm^{-1} when coordinated to a Na^{+} ion.[36] For a deprotonated carboxylic acid (carboxylate), on the other hand, the strong band for the anti-symmetric stretching mode is found at 1620–1640 cm^{-1} and the weaker band for the symmetric stretching mode is typically located at 1300–1400 cm^{-1}.[37,38] In the IR spectra of all serine clusters investigated here (see Fig. 2), the strongest band occurs at around 1640 cm^{-1} and no bands at higher wavenumber are observed, which implies that all carboxylic acid groups are deprotonated, all amine groups are protonated and the molecules in all clusters are thus zwitterionic.

Most importantly, for homochiral $(Ser_8Cl_2)^{2-}$ all bands are narrow. This implies that all oscillators are in a similar environment and that the complex must have a highly symmetric structure. These narrow bands are in contrast to the IR spectra of the larger species $(Ser_{10}Cl_2)^{2-}$ and $(Ser_{12}Cl_2)^{2-}$ and heterochiral $(Ser_8Cl_2)^{2-}$ where the bands occur at similar positions, indicating zwitterionic species, but with significantly increased width. This broadening is almost certainly caused by local variations in the interactions of the oscillators with their surroundings, indicative of structures with low symmetry. Further, for $(Ser_{10}Cl_2)^{2-}$ and $(Ser_{12}Cl_2)^{2-}$, there is no difference in cross section

(see Fig. 2a and b) or IR spectra between enantiomerically pure and statistically mixed L- and D-Ser clusters. This indicates that $(Ser_{10}Cl_2)^{2-}$ and $(Ser_{12}Cl_2)^{2-}$ as well as heterochiral $(Ser_8Cl_2)^{2-}$ are non-specific assemblies of zwitterionic serine.

For $(Ser_8Cl_2)^{2-}$, a structure for its compact form must fulfill several requirements: a) it has to have a strong preference for homochirality, i.e. changing the chirality of one or more amino acid units destabilizes the structure; b) the structure has to be compact and its calculated cross section needs to match the experimental cross section; c) it has to consist purely of zwitterionic amino acid units; d) the structure has to have an intrinsic preference for two chloride ions, not just one; e) the stability should be exceptionally high and all possible hydrogen bonds should be saturated; f) it should be specific to eight amino acid units and not easily add additional units; g) the symmetry should be high in order to yield narrow bands in the IR spectrum, and finally h) the theoretically calculated IR spectrum should match the experimental spectrum.

In principle, a global search for suitable structures that fulfill the above requirements can be done. However, since the conformation space is huge and accurate calculations of the energy are expensive, such an approach is impractical. Therefore, we instead derived a structure guided by chemical intuition as well as by structures suggested previously.[8,19-21] The resulting structure, optimized at the PBE0/cc-pVTZ level and including Grimme's D3 dispersion correction,[39] is shown from several perspectives in Fig. 3. The structure is compact and has a theoretical CCS of 192 Å^2, which compares well to the experimental value for the homochiral species of 189 Å^2. All eight Ser molecules are equivalent by symmetry and the point group is D_4. The structure can be thought of as consisting of two layers, with each layer consisting of a ring of four molecules that interact via hydrogen bonding of the $-NH_3^+$ group and -OH sidechain with the $-COO^-$ group of the next molecule. Between the two layers, the sense of rotation is reversed and the two layers are secured to each other via $-NH_3^+-$ $^-OOC-$ salt bridges. The $-NH_3^+$ groups point slightly to the center and form a cavity that holds the two chloride ions, whose distance from each other is only 3.96 Å (see Fig. 3). The xyz-coordinates of this structure is given in Supplementary Table 2. The binding of the chloride ions is quite strong and calculations show that the adiabatic removal of the first chloride ion requires 52 kcal/mol and that of both ions 169 kcal/mol of energy. The Gibbs free

energy of reaction (298 K) for gas phase assembly of the structure from eight serine units and two chloride ions is calculated to be −106 kcal mol^{-1} (see Supplementary Tables 3 and 4).

Figure 3b) shows the experimental IR spectrum of homochiral $(Ser_8Cl_2)^{2-}$ together with the calculated IR spectrum. Clearly, the match is very good in both peak positions as well as relative intensitiy. At the highest frequency of 1639 cm^{-1}, the band for the asymmetric-stretch mode of the -COO$^-$ group can be found, which is coupled to bending modes of the -NH$_3^+$ group. The three additional bands at 1616 cm^{-1}, 1583 cm^{-1}, and 1496 cm^{-1} arise from bending modes in the -NH$_3^+$ group. The two strong bands slightly below 1400 cm^{-1} stem from the symmetric stretching modes of the -COO$^-$ group. Finally, a band is found at 1070 cm^{-1}, which is red-shifted to 1059 cm^{-1} in the experiment and arises from the C–OH stretch motions in the side chains. Experimental and theoretical IR spectra of $(Ser_8Cl_2)^{2-}$ with isotopic substitutions further confirm the proposed structure (See Supplementary Fig. 1).

The cluster structure shown in Fig. 3 has D_4 symmetry in which all serine molecules are equivalent and which is the highest symmetry possible for a cluster of that composition. This also means that changing the chirality of one amino acid breaks the symmetry, leaves at least one functional group without a hydrogen bonding partner, and disrupts the hydrogen bonding pattern in one of the two rings. Changing the chirality of all four units in one of the rings changes its sense or rotation and thereby alters the interaction between those rings. Thus, the structure has a strong preference for homochirality. The high symmetry of the structure also implies that, since all monomer units are equivalent, all vibrational oscillators are equivalent as well, which explains why the bands in the IR spectrum are so narrow. The cavity in the structure is nicely suited to accept two negatively charged ions. The diameter of the cavity is ~4.25 Å which is determined by the distance between two opposite hydrogen atoms of -NH$_3^+$ groups directed at the center (Fig 3c). In the equilibrium structure, the distance between two chloride ions is 3.96 Å. One can compare those numbers to the diameter of a chloride or bromide ion of ~3.34 Å and ~3.64 Å, respectively,[40] and conclude that the cavities are large enough to support those ions. An iodine ion on the other hand has an ionic diameter of 4.12 Å,[40] too large to fit into the cavities without

9

distorting them. This is in line with the observation of "magic" $(Ser_8Cl_2)^{2-}$ and $(Ser_8Br_2)^{2-}$ but the absence of a corresponding iodine-containing counterpart.[18]

The structure for $(Ser_8Cl_2)^{2-}$ is very special, can only exist for serine and only for clusters with eight monomer units. It does not offer suitable docking sites for the addition of further amino acid units, making the structure unreactive for further growth. An important question is, to what degree can the structure of this anionic cluster be transferable to neutral or cationic clusters? Clearly, the size and electrostatic environment of the cavities are geared towards anions and specifically, towards holding two of them. Removing those anions to generate a neutral structure will cause significant destabilization. For cationic species, the Serine octamer is observed to be "magic" either singly protonated or complexed with a single alkali ion. The anionic structure shown here will not easily accommodate those positive charges and it is not clear if the cationic serine octamer complexes bear any resemblance to the anionic one.

Does the $(Ser_8Cl_2)^{2-}$ complex also exists in the condensed phase? A search for the protonated serine octamer in aqueous solution using IR and NMR was unsuccessful.[41] In the current experiment, ions are sampled via nano-ESI. Provided that the experimental conditions are soft enough, even weakly bound complexes can be transferred to the gas phase and through the instrument. In addition, however, in the ESI process complexes can assemble non-specifically during droplet evaporation. Disentangling these processes is generally difficult. There are, however, several points that speak against a non-specific assembly of the homochiral $(Ser_8Cl_2)^{2-}$ cluster during the ESI process and indicate that this complex might very well exist in solution. First, in a non-specific aggregation scenario, smooth mass distributions would be expected but mass spectra (Fig. 1) do not show such behavior. Second, fragmentation might occur during and after the ESI process. If this occurs clusters containing less than eight serine units would be expected to be present, but they are not observed. Further, we exclusively observe complexes containing two and three chloride ions and in a non-specific aggregation scenario, complexes containing just one chloride ion would be expected to be present as well. However, while the above arguments are suggestive that homochiral $(Ser_8Cl_2)^{2-}$ might be present in solution, they are

not conclusive. Further studies are needed to unambiguously prove this special complex exists in solution.

Materials and methods

Sample preparations. All solvents, hydrochloric acid, L-serine and D-serine were purchased from Sigma-Aldrich (Taufkirchen, Germany). L-Serine-2,3,3-D$_3$,^{13}C$_3$,^{15}N (L-Ser*) was obtained from Cambridge Isotope Laboratories (Tewksbury, MA, USA). All sample solutions were prepared in water with a total serine concentration of 10 mM and a hydrochloric acid concentration of 1 mM.

Ion mobility spectrometry-mass spectrometry (IMS-MS) coupled to infrared multiple photon dissociation (IRMPD) spectroscopy. A home-built hybrid drift-tube quadrupole time-of-flight mass spectrometer equipped with nanoelectrospray source was used for this work. The instrumental details are described elsewhere.[25,42-44] A small aliquot (5–10 μL) of sample solution was loaded on a Pd/Pt-coated borosilicate emitter and electrosprayed into the instrument. The spray voltage was –1.0 kV to generate negatively charged ions. Ions are collected in an ion funnel, pulsed into a 80-cm-long drift tube, and drift through helium buffer gas (4–5 mbar) under the influence of a weak electric field (10–15 V cm^{-1}). Ions are separated as their drift velocities depend on their sizes and charges. At the end of the drift tube, a second ion funnel collects and transfers ions into the high vacuum region. By varying the timing of a high voltage pulse (–4.5 kV), which pulses a fraction of ion mobility-separated ions into orthogonal TOF, a drift time-selected TOF mass spectrum is recorded in the drift time range 5–14 ms. The arrival time distribution (ATD) is constructed by extracting the drift time-dependent ion current of specific *m/z* ions. Collision cross-sections are determined using the measured drift time and the Mason-Schamp equation.[45] For measuring size- and conformer-selective infrared spectra, a narrow fraction of ions is selected by electrostatic deflection after ion mobility separation and *m/z* selection is done in a quadrupole mass filter. The ion mobility- and *m/z*-selected ions are then irradiated by infrared photons from the Fritz Haber Institute free electron laser (FHI FEL).[46] When the photon energy of the IR light is in resonance with an infrared active vibration of the ion, the absorption of multiple photons and subsequent dissociated can occur. The abundances of

11

precursor and fragment ions are recorded using the TOF mass analyzer. Fragment TOF mass spectra obtained with low and high laser fluence are shown in Supplementary Fig. 4. IR spectra are obtained by scanning the laser in 3 cm^{-1} step in the range 1000–1900 cm^{-1} and plotting the fragmentation efficiency as a function of wavenumber.

Calculation Details. The initial geometry of doubly-chlorinated homochiral serine octamer was generated and pre-optimized with the OPLS3 force field using MacroModel.[47] The pre-optimized structure was further optimized using Gaussian09[48] at the PBE0 level of density functional theory using the cc-pVTZ basis set and Grimme D3 dispersion corrections.[39] Harmonic vibrational frequencies were calculated from the optimized structure, scaled by 0.957,[49] and convoluted with Gaussian functions of 10 cm^{-1} bandwidth to construct the theoretical infrared spectrum. The theoretical collision cross-section of the optimized structure was calculated using the trajectory method.[50] For the energetics, counterpoise calculations were performed to estimate the effect of basis set superposition error (BSSE) (see Supplementary Table 4 in the Supplementary Information).

Data availability

The data that support the findings of this study are available from the authors on reasonable request.

Author contributions

J.S., S.W., K.P., M.T.B. and G.v.H. conceived and designed the experiments: J.S., S.W. performed the experiments: J.S. analyzed the data and suggested the structure of the serine octamer with two chlorides. All authors co-wrote the paper.

Additional information

Supplementary information is available in the online version of the paper. Reprints and permissions information is available online at www.nature.com/reprints. Correspondence and requests for materials should be addressed to J.S. and G.v.H..

Competing financial interest

The Authors declare no competing financial interest.

References

1   O. Echt, K. Sattler & E. Recknagel. Magic numbers for sphere packings - experimental-verification in free xenon clusters. *Phys. Rev. Lett.* **47**, 1121-1124 (1981).
2   H. W. Kroto, J. R. Heath, S. C. O'Brian, R. F. Curl & R. E. Smalley. C_{60} - Buckminsterfullerene. *Nature* **318**, 162-163 (1985).
3   B. C. Guo, S. Wei, J. Purnell, S. Buzza & A. W. Castleman. Metallo-Carbohedrenes $[M_8C_{12}^+$ (M = V, Zr, Hf, and Ti)] - a Class of Stable Molecular Cluster Ions. *Science* **256**, 515-516 (1992).
4   J. Li, X. Li, H. J. Zhai & L. S. Wang. Au_{20}: A tetrahedral cluster. *Science* **299**, 864-867 (2003).
5   P. Gruene, D. M. Rayner, B. Redlich, A. F. van der Meer, J. T. Lyon, G. Meijer & A. Fielicke. Structures of neutral Au_7, Au_{19}, and Au_{20} clusters in the gas phase. *Science* **321**, 674-676 (2008).
6   M. Miyazaki, A. Fujii, T. Ebata & N. Mikami. Infrared spectroscopic evidence for protonated water clusters forming nanoscale cages. *Science* **304**, 1134-1137 (2004).
7   J. W. Shin, N. I. Hammer, E. G. Diken, M. A. Johnson, R. S. Walters, T. D. Jaeger, M. A. Duncan, R. A. Christie & K. D. Jordan. Infrared signature of structures associated with the $H^+(H_2O)_n$ (n = 6 to 27) clusters. *Science* **304**, 1137-1140 (2004).
8   R. G. Cooks, D. Zhang, K. J. Koch, F. C. Gozzo & M. N. Eberlin. Chiroselective self-directed octamerization of serine: Implications for homochirogenesis. *Anal. Chem.* **73**, 3646-3655 (2001).
9   P. Nemes, G. Schlosser & K. Vékey. Amino acid cluster formation studied by electrospray ionization mass spectrometry. *J. Mass Spectrom.* **40**, 43-49 (2005).
10 M. Kellermeier, R. Rosenberg, A. Moise, U. Anders, M. Przybylski & H. Colfen. Amino acids form prenucleation clusters: ESI-MS as a fast detection method in comparison to analytical ultracentrifugation. *Faraday Discuss.* **159**, 23-45 (2012).
11 L. Feketeová, G. N. Khairallah, C. Brunet, J. Lemoine, R. Antoine, P. Dugourd & R. A. J. O'Hair. Fragmentation of the tryptophan cluster $[Trp_9-2H]^{2-}$ induced by different activation methods. *Rapid Commun. Mass Spectrom.* **24**, 3255-3260 (2010).

12   A. E. Counterman & D. E. Clemmer. Anhydrous polyproline helices and globules. *J. Phys. Chem. B* **108**, 4885-4898 (2004).

13   R. R. Julian, R. Hodyss & J. L. Beauchamp. Salt bridge stabilization of charged zwitterionic arginine aggregates in the gas phase. *J. Am. Chem. Soc.* **123**, 3577-3583 (2001).

14   T. D. Do, N. E. C. de Almeida, N. E. LaPointe, A. Chamas, S. C. Feinstein & M. T. Bowers. Amino acid metaclusters: Implications of growth trends on peptide self-assembly and structure. *Anal. Chem.* **88**, 868-876 (2016).

15   S. C. Nanita, Z. Takats, R. G. Cooks, S. Myung & D. E. Clemmer. Chiral enrichment of serine via formation, dissociation, and soft-landing of octameric cluster ions. *J. Am. Soc. Mass. Spectrom.* **15**, 1360-1365 (2004).

16   S. C. Nanita & R. G. Cooks. Serine octamers: cluster formation, reactions, and implications for biomolecule homochirality. *Angew. Chem. Int. Ed.* **45**, 554-569 (2006).

17   K. J. Koch, F. C. Gozzo, D. Zhang, M. N. Eberlin & R. G. Cooks. Serine octamer metaclusters: formation, structure elucidation and implications for homochiral polymerization. *Chem. Commun.*, 1854-1855 (2001).

18   S. C. Nanita & R. G. Cooks. Negatively-charged halide adducts of homochiral serine octamers. *J. Phys. Chem. B* **109**, 4748-4753 (2005).

19   C. A. Schalley & P. Weis. Unusually stable magic number clusters of serine with a surprising preference for homochirality. *Int. J. Mass Spectrom.* **221**, 9-19 (2002).

20   R. R. Julian, R. Hodyss, B. Kinnear, M. F. Jarrold & J. L. Beauchamp. Nanocrystalline aggregation of serine detected by electrospray ionization mass spectrometry: Origin of the stable homochiral gas-phase serine octamer. *J. Phys. Chem. B* **106**, 1219-1228 (2002).

21   A. E. Counterman & D. E. Clemmer. Magic number clusters of serine in the gas phase. *J. Phys. Chem. B* **105**, 8092-8096 (2001).

22   D. E. Clemmer & M. F. Jarrold. Ion mobility measurements and their applications to clusters and biomolecules. *J. Mass Spectrom.* **32**, 577-592 (1997).

23   T. Wyttenbach & M. T. Bowers. Gas-phase conformations: The ion mobility/ion chromatography method. *Modern Mass Spectrometry* **225**, 207-232 (2003).

24   A. B. Kanu, P. Dwivedi, M. Tam, L. Matz & J. Hill, Herbert H. Ion mobility-mass spectrometry. *J. Mass Spectrom.* **43**, 1-22 (2008).

25   S. Warnke, J. Seo, J. Boschmans, F. Sobott, J. H. Scrivens, C. Bleiholder, M. T. Bowers, S. Gewinner, W. Schöllkopf, K. Pagel & G. von Helden. Protomers of Benzocaine: Solvent and Permittivity Dependence. *J. Am. Chem. Soc.* **137**, 4236-4242 (2015).

26   A. Masson, M. Z. Kamrath, M. A. S. Perez, M. S. Glover, U. Rothlisberger, D. E. Clemmer & T. R. Rizzo. Infrared Spectroscopy of Mobility-Selected H+-Gly-Pro-Gly-Gly (GPGG). *J. Am. Soc. Mass. Spectrom.* **26**, 1444-1454 (2015).

27   J. Seo, S. Warnke, S. Gewinner, W. Schöllkopf, M. T. Bowers, K. Pagel & G. von Helden. The impact of environment and resonance effects on the site of protonation of aminobenzoic acid derivatives. *Phys. Chem. Chem. Phys.* **18**, 25474-25482 (2016).

28   L. Voronina, A. Masson, M. Kamrath, F. Schubert, D. Clemmer, C. Baldauf & T. Rizzo. Conformations of Prolyl–Peptide Bonds in the Bradykinin 1–5 Fragment in Solution and in the Gas Phase. *J. Am. Chem. Soc.* **138**, 9224-9233 (2016).

29   J. Seo, W. Hoffmann, S. Warnke, X. Huang, S. Gewinner, W. Schöllkopf, M. T. Bowers, G. von Helden & K. Pagel. An infrared spectroscopy approach to follow β-sheet formation in peptide amyloid assemblies. *Nature Chemistry*, (in press) (2016).

30   X. Kong, I. A. Tsai, S. Sabu, C.-C. Han, Y. T. Lee, H.-C. Chang, S.-Y. Tu, A. H. Kung & C.-C. Wu. Progressive stabilization of zwitterionic structures in $[H(Ser)_{2-8}]^+$ studied by infrared photodissociation spectroscopy. *Angew. Chem. Int. Ed.* **45**, 4130-4134 (2006).

31   X. Kong, C. Lin, G. Infusini, H.-B. Oh, H. Jiang, K. Breuker, C.-C. Wu, O. P. Charkin, H.-C. Chang & F. W. McLafferty. Numerous isomers of serine octamer ions characterized by infrared photodissociation spectroscopy. *ChemPhysChem* **10**, 2603-2606 (2009).

32   F. X. Sunahori, G. Yang, E. N. Kitova, J. S. Klassen & Y. Xu. Chirality recognition of the protonated serine dimer and octamer by infrared multiphoton dissociation spectroscopy. *Phys. Chem. Chem. Phys.* **15**, 1873-1886 (2013).
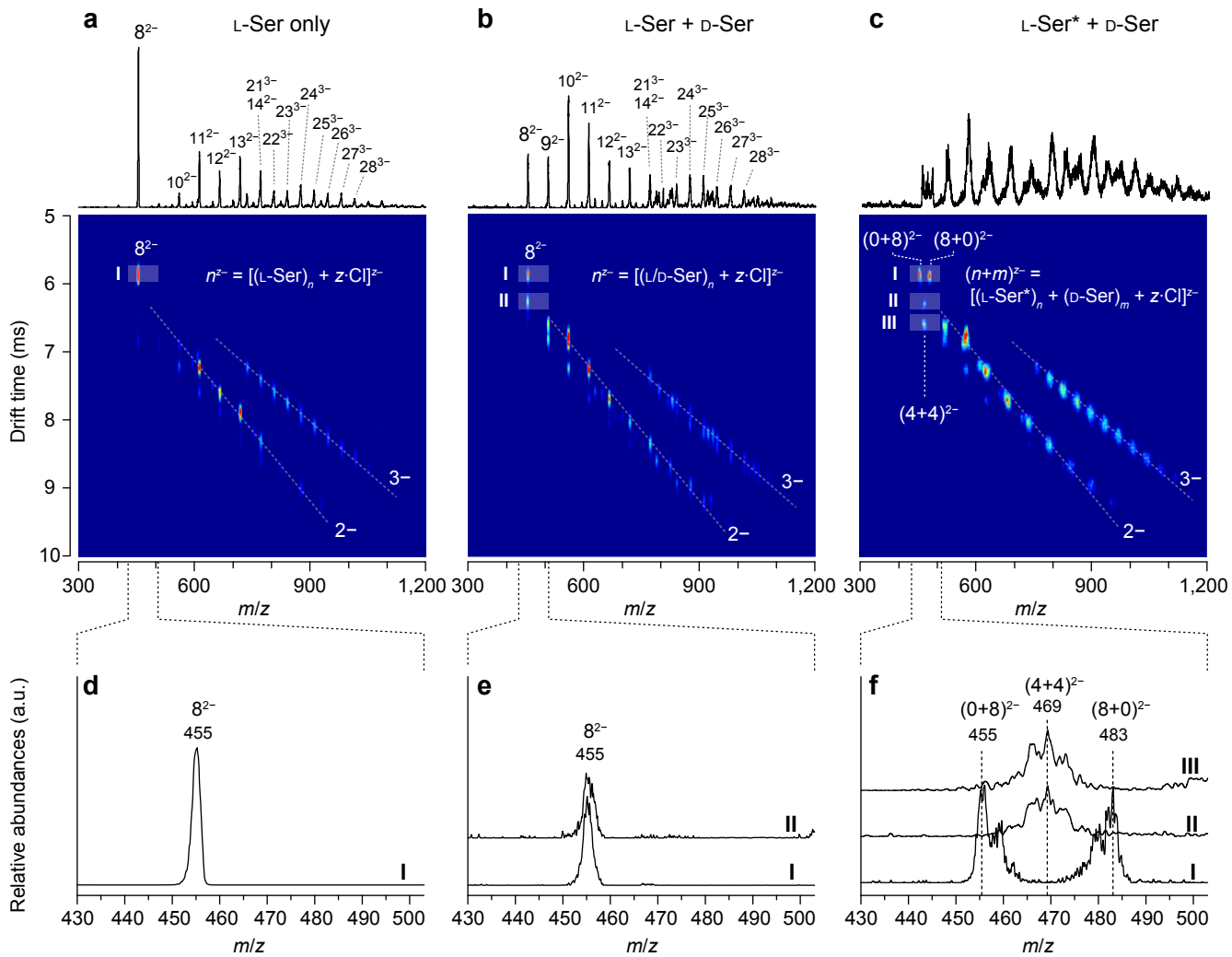
33   Z. Takats, S. C. Nanita, G. Schlosser, K. Vekey & R. G. Cooks. Atmospheric pressure gas-phase H/D exchange of serine octamers. *Anal. Chem.* **75**, 6147-6154 (2003).

34   R. Linder, K. Seefeld, A. Vavra & K. Kleinermanns. Gas phase infrared spectra of nonaromatic amino acids. *Chem. Phys. Lett.* **453**, 1-6 (2008).

35   J. Antony, G. von Helden, G. Meijer & B. Schmidt. Anharmonic midinfrared vibrational spectra of benzoic acid monomer and dimer. *J. Chem. Phys.* **123**, 014305 (2005).

36   C. Kapota, J. Lemaire, P. Maitre & G. Ohanessian. Vibrational signature of charge solvation vs salt bridge isomers of sodiated amino acids in the gas phase. *J. Am. Chem. Soc.* **126**, 1836-1842 (2004).

37   J. Oomens, J. D. Steill & B. Redlich. Gas-phase IR spectroscopy of deprotonated amino acids. *J. Am. Chem. Soc.* **131**, 4310-4319 (2009).

38   M. N. Blom, I. Compagnon, N. C. Polfer, G. von Helden, G. Meijer, S. Suhai, B. Paizs & J. Oomens. Stepwise solvation of an amino acid: The appearance of zwitterionic structures. *J. Phys. Chem. A* **111**, 7309-7316 (2007).

39   S. Grimme, J. Antony, S. Ehrlich & H. Krieg. A consistent and accurate ab initio parametrization of density functional dispersion correction (DFT-D) for the 94 elements H-Pu. *J. Chem. Phys.* **132**, 154104 (2010).

40   R. Shannon. Revised effective ionic radii and systematic studies of interatomic distances in halides and chalcogenides. *Acta Cryst. A* **32**, 751-767 (1976).

41   S. Vandenbussche, G. Vandenbussche, J. Reisse & K. Bartik. Do Serine Octamers Exist in Solution? Relevance of this Question in the Context of the Origin of Homochirality on Earth. *Eur. J. Org. Chem.* **2006**, 3069-3073 (2006).

42   P. R. Kemper, N. F. Dupuis & M. T. Bowers. A new, higher resolution, ion mobility mass spectrometer. *Int. J. Mass Spectrom.* **287**, 46-57 (2009).

43   S. Warnke, C. Baldauf, M. T. Bowers, K. Pagel & G. von Helden. Photodissociation of Conformer-Selected Ubiquitin Ions Reveals Site-Specific Cis/Trans Isomerization of Proline Peptide Bonds. *J. Am. Chem. Soc.* **136**, 10308-10314 (2014).

44   S. Warnke, G. von Helden & K. Pagel. Analyzing the higher order structure of proteins with conformer-selective ultraviolet photodissociation. *Proteomics* **15**, 2804-2812 (2015).

45   E. A. Mason & E. W. McDaniel. *Transport Properties of Ions in Gases*. (Wiley-VCH, 2005).

46   W. Schöllkopf, S. Gewinner, H. Junkes, A. Paarmann, G. von Helden, H. Bluem & A. M. M. Todd. in *Advances in X-Ray Free-Electron Lasers Instrumentation III* Vol. 9512 *Proceedings of SPIE* (ed S. G. Biedron) (2015).

47   Macromodel (Schödinger, LLC, New York, NY, USA, 2016).

48   Gaussian 09, Revision D.01 (Gaussian, Inc., Wallingford, CT, USA, 2009).

49   M. K. Kesharwani, B. Brauer & J. M. L. Martin. Frequency and Zero-Point Vibrational Energy Scale Factors for Double-Hybrid Density Functionals (and Other Selected Methods): Can Anharmonic Force Fields Be Avoided? *J. Phys. Chem. A* **119**, 1701-1714 (2015).

50   M. F. Mesleh, J. M. Hunter, A. A. Shvartsburg, G. C. Schatz & M. F. Jarrold. Structural Information from Ion Mobility Measurements: Effects of the Long-Range Potential. *J. Phys. Chem.* **100**, 16082-16086 (1996).
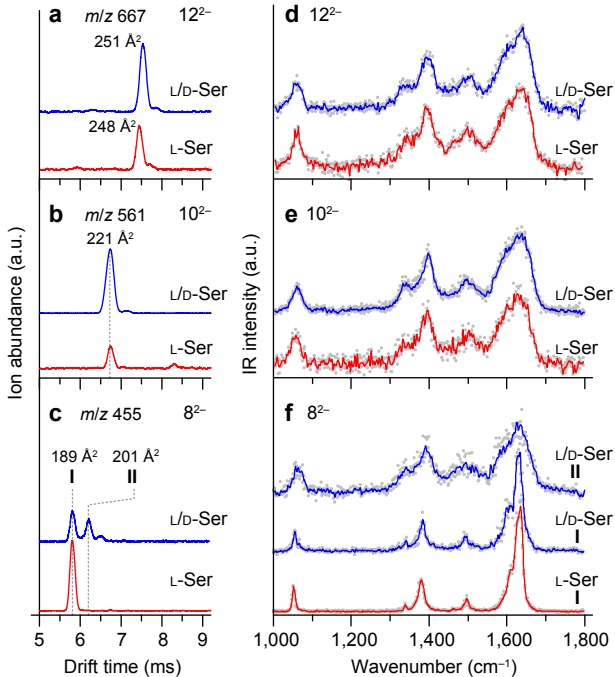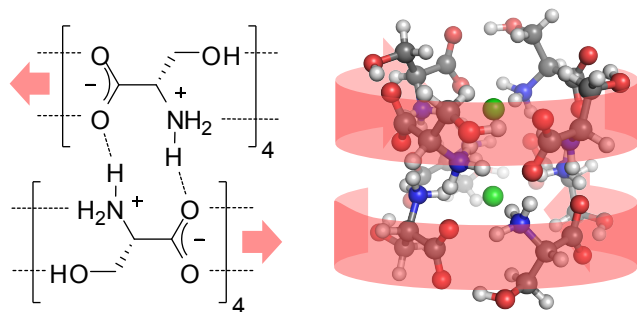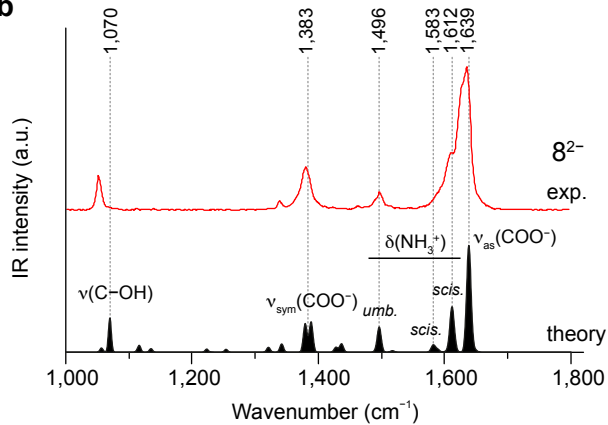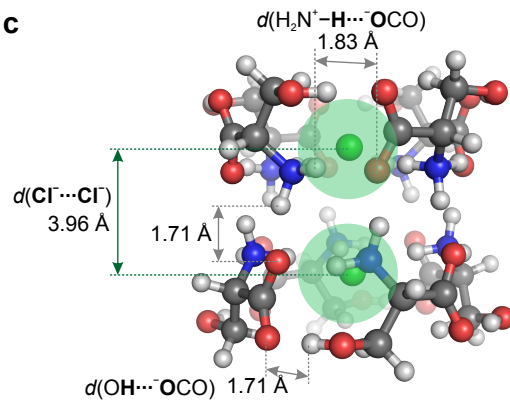
Figure Captions

Figure 1: Ion mobility spectrometry-mass spectrometry of serine cluster anions. Time-of-flight (TOF) mass spectra of aqueous solutions of **a**, L-Ser and HCl; **b**, 1:1 mixture of L- and D-Ser and HCl and **c**, 1:1 mixture of D-Ser and L-Ser* and HCl where L-Ser* is L-serine-D_3,$^{13}C_3$,$^{15}N_1$. The notation n^{z-} stands for $[n\mathrm{Ser} + z\mathrm{Cl}]^{z-}$. The distributions of serine clusters complexed with two and three chloride ions are marked by dashed lines in the drift time versus m/z plots. **d,e,f**, drift time-selected TOF mass spectra highlighting octamer-dichloride complexes with three drift time windows; 5.8–6.0 ms (**I**), 6.3–6.5 ms (**II**), and 6.6–6.8 ms (**III**).

Figure 2: Size- and conformer-selected infrared spectra of serine cluster-dichloride complexes. a,b,c Arrival time distributions and corresponding collision cross-sections of $(\mathrm{Ser}_{12}\mathrm{Cl}_2)^{2-}$ (**a**), $(\mathrm{Ser}_{10}\mathrm{Cl}_2)^{2-}$ (**b**), and $(\mathrm{Ser}_8\mathrm{Cl}_2)^{2-}$ (**c**). Red and blue traces denote the results from L-Ser only and racemic Ser, respectively. For $(\mathrm{Ser}_8\mathrm{Cl}_2)^{2-}$, the smaller (CCS = 189 Å^2) and larger (CCS = 201 Å^2) conformers are annotated by **I** and **II**, respectively. **d,e,f** Infrared spectra of $(\mathrm{Ser}_{12}\mathrm{Cl}_2)^{2-}$ (**d**), $(\mathrm{Ser}_{10}\mathrm{Cl}_2)^{2-}$ (**e**), and $(\mathrm{Ser}_8\mathrm{Cl}_2)^{2-}$ (**f**). Gray dots are data points from two repeated scans and the lines denote averaged results.

Figure 3: Theoretical structure of the homochiral serine octamer-dichloride complex. a Proposed symmetric (D_4 point group) homochiral structure of the serine octamer-dichloride complex. **b** Theoretical IR bands of the proposed structure compared with the experimental results. Symmetric and antisymmetric stretching vibrations (ν_{sym} and ν_{as}) of the carboxylate groups ($-\mathrm{COO}^-$) as well as deformations (δ) of protonated amine groups ($-\mathrm{NH}_3^+$) are assigned. The notations '*umb.*' and '*scis.*' denote umbrella and scissoring modes. **c,d** Detailed views of the octamer from side (**c**) and top (**d**). The ionic size of chloride anion is illustrated by the larger green circle.

a L-Ser only

8^{2-}

10^{2-} 11^{2-} 12^{2-} 13^{2-} 14^{2-} 21^{3-} 22^{3-} 23^{3-} 24^{3-} 25^{3-} 26^{3-} 27^{3-} 28^{3-}

8^{2-}

I

$n^{z-} = [(\text{L-Ser})_n + z \cdot \text{Cl}]^{z-}$

3−

2−

b L-Ser + D-Ser

10^{2-} 11^{2-}

8^{2-} 9^{2-} 12^{2-} 13^{2-} 14^{2-} 21^{3-} 22^{3-} 23^{3-} 24^{3-} 25^{3-} 26^{3-} 27^{3-} 28^{3-}

8^{2-}

I
II

$n^{z-} = [(\text{L/D-Ser})_n + z \cdot \text{Cl}]^{z-}$

3−

2−

c L-Ser* + D-Ser

$(0+8)^{2-}$ $(8+0)^{2-}$

I
II
III

$(n+m)^{z-} = [(\text{L-Ser*})_n + (\text{D-Ser})_m + z \cdot \text{Cl}]^{z-}$

$(4+4)^{2-}$

3−

2−

Drift time (ms)

m/z

d

8^{2-}
455

I

e

8^{2-}
455

II

I

f

$(0+8)^{2-}$
455

$(4+4)^{2-}$
469

$(8+0)^{2-}$
483

III

II

I

Relative abundances (a.u.)

m/z

a m/z 667 12^{2-}
251 Å²
L/D-Ser
248 Å²
L-Ser

b m/z 561 10^{2-}
221 Å²
L/D-Ser
L-Ser

c m/z 455 8^{2-}
189 Å²   201 Å²
I   II
L/D-Ser
L-Ser

d 12^{2-}
L/D-Ser
L-Ser

e 10^{2-}
L/D-Ser
L-Ser

f 8^{2-}
L/D-Ser II
L/D-Ser I
L-Ser I

Ion abundance (a.u.)
IR intensity (a.u.)
Drift time (ms)
Wavenumber (cm⁻¹)

a

b

8^{2-}
exp.

ν(C−OH)

ν_{sym}(COO⁻)   *umb.*

δ(NH$_3^+$)

scis.

scis.

ν_{as}(COO⁻)

theory

Wavenumber (cm⁻¹)

IR intensity (a.u.)

1,070 1,383 1,496 1,583 1,612 1,639

c

d(H$_2$N⁺−**H**···⁻**O**CO)
1.83 Å

d(**Cl**⁻···**Cl**⁻)
3.96 Å

1.71 Å

d(O**H**···⁻**O**CO) 1.71 Å

d

$2 \cdot r_{ion}$(Cl⁻)
3.34 Å

d(H$_2$N⁺−**H**···**H**−⁺NH$_2$)
4.25 Å